Accepted Manuscript

Title: Simultaneous determination of Paraquat and Atrazine in water samples with a White Light Reflectance Spectroscopy biosensor

Authors: Eleftheria Stavra, Panagiota S. Petrou, Georgios Koukouvinos, Christos Kiritsis, Ioannis Pirmettis, Minas Papadopoulos, Dimitrios Goustouridis, Anastasios Economou, Konstantinos Misiakos, Ioannis Raptis, Sotirios E. Kakabakos

PII: S0304-3894(18)30546-6
DOI: https://doi.org/10.1016/j.jhazmat.2018.07.029
Reference: HAZMAT 19537

To appear in: *Journal of Hazardous Materials*

Received date: 16-4-2018
Revised date: 4-7-2018
Accepted date: 6-7-2018

Please cite this article as: Stavra E, Petrou PS, Koukouvinos G, Kiritsis C, Pirmettis I, Papadopoulos M, Goustouridis D, Economou A, Misiakos K, Raptis I, Kakabakos SE, Simultaneous determination of Paraquat and Atrazine in water samples with a White Light Reflectance Spectroscopy biosensor, *Journal of Hazardous Materials* (2018), https://doi.org/10.1016/j.jhazmat.2018.07.029

Simultaneous determination of Paraquat and Atrazine in water samples with a White Light Reflectance Spectroscopy biosensor

Eleftheria Stavra[a,b], Panagiota S. Petrou[a*], Georgios Koukouvinos[a], Christos Kiritsis[c], Ioannis Pirmettis[c], Minas Papadopoulos[c], Dimitrios Goustouridis[d,e], Anastasios Economou[b], Konstantinos Misiakos[f], Ioannis Raptis[d], Sotirios E. Kakabakos[a*]

[a]Immunoassays-Immunosensors Lab, INRASTES, NCSR "Demokritos", 15341 Aghia Paraskevi, Greece

[b]Analytical Chemistry Lab, Department of Chemistry, University of Athens, Panepistimiopolis 15771 Zografou, Greece

[c]Radiopharmaceuticals Lab, INRASTES, NCSR "Demokritos", 15341 Aghia Paraskevi, Greece

[d]ThetaMetrisis S.A., Polydefkous 14, 12243 Egaleo, Greece

[e]Electronics Department, TEI of Piraeus, 12244 Egaleo, Greece

[f]Institute of Nanoscience & Nanotechnology, NCSR "Demokritos", 15341 Aghia Paraskevi, Greece

Corresponding author: Panagiota Petrou

Immunoassays/Immunosensors Lab
Institute of Nuclear & Radiological Sciences & Technology, Energy & Safety
NCSR "Demokritos"
GR-15310 Aghia Paraskevi
Greece
Tel. +302106503819, Fax. +302106543526

Graphical abstract

GRAPHICAL ABSTRACT

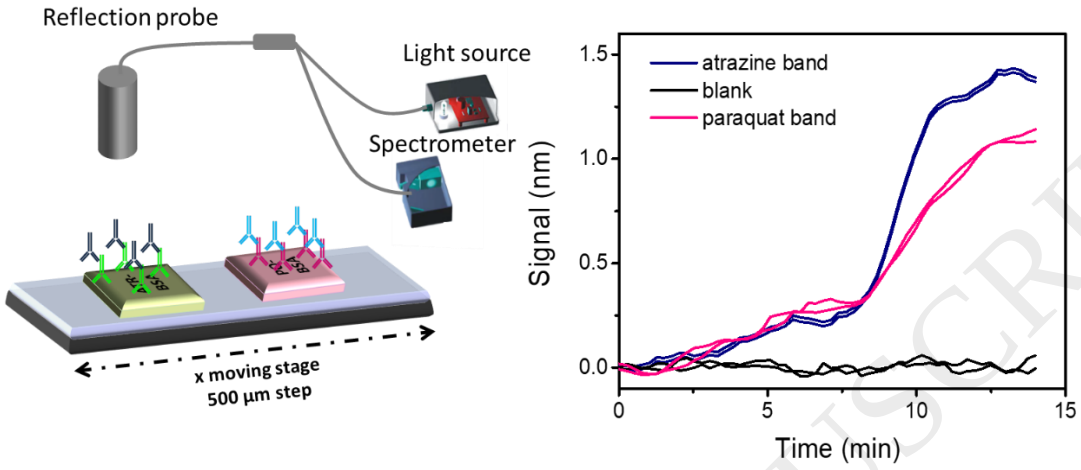

Highlights

- Optical immunosensor for label-free detection of paraquat and atrazine in water samples
- The two pesticides are simultaneously determined in 12 min
- The LODs are lower from the MRLs for the two pesticides set by EU
- Bottled and tap water samples can be analysed without any pre-treatment

Abstract

An optical immunosensor based on White Light Reflectance Spectroscopy for the simultaneous determination of the herbicides atrazine and paraquat in drinking water samples is demonstrated. The biosensor allows for the label-free real-time monitoring of biomolecular interactions taking place onto a SiO_2/Si chip by transforming the shift in the reflected interference spectrum due to reaction to effective biomolecular layer thickness. Dual-analyte determination is accomplished by functionalizing spatially distinct areas of the chip with protein conjugates of the two herbicides and scanning the surface with an optical reflection probe. A competitive immunoassay format was adopted, followed by reaction with secondary

antibodies for signal enhancement. The sensor was highly sensitive with detection limits of 40 and 50 pg/mL for paraquat and atrazine, respectively, and the assay duration was 12 min. Recovery values ranging from 90.0 to 110% were determined for the two pesticides in spiked bottled and tap water samples, demonstrating the sensor accuracy. In addition, the sensor could be regenerated and re-used at least 20 times without significant effect on the assay characteristics. Its excellent analytical performance and short analysis time combined with the small sensor size should be helpful for fast on-site determinations of these analytes.

Keywords: Paraquat; Atrazine; White Light Reflectance Spectroscopy; Label-free biosensor; Drinking water

1. Introduction

Nowadays, the necessity for devices endowed with excellent analytical performance and portability for on-site applications is becoming more and more evident [1]. To this direction several types of biosensors have been exploited as alternatives to conventional instrumental analytical techniques for a wide range of applications, including the determination of pesticides in water, food or feed samples [2-4].

Broad spectrum synthetic pesticides have been extensively used worldwide in agricultural practice due to their beneficial effects in crop protection and agricultural economy [5]. Nevertheless, their excessive use in combination with their bioaccumulation capabilities has been considered responsible for irreversible effects in human health and the ecosystems [6]. In order to harmonize the necessity for pesticide usage and the obligation to protect human health and the environment, the regulatory bodies in European Union [7] as well as in other countries worldwide have set a frame for pesticides management, including the maximum allowable

limits of various pesticides in foods and beverages as well as a list of substances for which manufacturing, use and distribution is banned within their borders.

Paraquat and atrazine are two examples of herbicides banned within EU since 2007 and 2004, respectively (Judgment of the Court of First Instance Case T-229/04, 2007; Commission decision of 10 March 2004, Official Journal of the European Union, 2004). Nonetheless, they are still used in USA and in a lot of countries worldwide. Paraquat is highly toxic for humans and animals [8] and recent studies have associated exposure to paraquat with Parkinson's disease [9, 10]. Several methods have been reported in the literature for the determination of paraquat in water, food and environmental samples or even biological fluids such as serum. These methods include HPLC coupled to UV or mass spectrometry detectors [11-15], immunoassays [19, 20], and sensors [18-26]. Atrazine, though not as toxic as paraquat, has been banned within EU due to its ability to remain for long periods in soil and groundwater [27, 28]. Although several studies has shown that atrazine is an endocrine disruptor to both animals and humans [28], it remains one of the most commonly used herbicides in many countries outside EU. Therefore, a large number of methods has been developed for atrazine detection, including classical chromatographic gas or liquid separation technics combined with a variety of detectors [29-32], immunoassays [33, 34], and sensors [29-49]. The latter present the only viable solution towards the development of devices for on-site determination of pesticides due to increased potential for miniaturization as compared to other instrumental methods of analysis. Among the various types of sensors, optical label-free biosensors offer unique advantages over those employing labels due to the absence of labelling which can alter the binding affinity, increase the analysis cost, and complicate the assay procedure moving away the potential for on-site determinations.

Optical label-free sensors can be in general categorized in two groups: refractometric and reflectrometric [50]. In the latter, the light is reflected by the different interfaces that create the transducer, usually including a dielectric material that acts as interference spacer. Binding reactions occurring at the dielectric material surface induce a layer thickness increase that affects the reflected beams leading to shift in the interference spectrum. The most common reflectrometric sensing method is reflectance interference spectroscopy, where the sensing element is a glass slide [50] or a planar silicon die [51] modified with a thin layer of transparent dielectric material (e.g., SiO_2). In addition, other substrates have been exploited, including porous silicon [52, 53] or other porous materials such as TiO_2 [54]. In general, sensing using porous materials relies on the increase of the refractive index of the porous photonic structure due to infiltration of the analytes into the pores. Thus, the surface porosity needs to be optimized with respect to analyte size, while when planar substrates are employed the same sensing surface could be used independently of the final application.

In the present work, a label-free sensor based on White Light Reflectance Spectroscopy (WLRS) for the fast simultaneous determination of paraquat and atrazine in water samples is presented. WLRS sensing approach has been already used for the immunochemical determination of high molecular weight analytes [51, 55] as well as for pesticides in wine samples [56]. The particular sensor allows for the label-free and real-time monitoring of biomolecular interactions by following the shift of the interference spectrum reflected from SiO_2/Si chip on the top surface of which the reactions takes place. Dual-analyte determination is accomplished by functionalizing spatially distinct areas of the chip with protein conjugates of the two herbicides and scanning the surface with an optical reflection probe (Fig. 1). A competitive immunoassay format was followed for both analytes, according to which mixtures of calibrators or samples with antibodies specific against the two herbicides were run over the chip, followed by reaction with secondary antibodies for signal enhancement (Fig. 1). Due to

lack of commercially available protein conjugates for paraquat, two conjugates with bovine serum albumin have been prepared and evaluated to select the most appropriate for use in the immunosensor. The cross-reactivity of the atrazine- and paraquat-specific antibodies towards each other as well as with respect to compounds with structural similarity was also evaluated. Finally, the accuracy of the determinations performed with the dual-analyte immunosensor was evaluated through recovery experiments in bottled and tap water samples.

2. Materials and Methods

2.1. Reagents

Four-inch Si wafers (<100>), purchased from Si-Mat Germany (Kaufering, Germany), were cleaned with acetone and isopropanol and then a 1000-nm thick SiO_2 layer was grown on them by thermal oxidation at 1100°C in the clean room facility of the Institute of Nanoscience and Nanotechnology of NCSR "Demokritos". The wafers were diced to chips with dimensions of 5mm x 15 mm. Bovine serum albumin (BSA), (3-aminopropy)-triethoxysilane (APTES), methyl-5-bromovalerate, methyl iodide, 4,4-dipyridyl, and cyanuric chloride were from Acros Organics (Geel, Belgium). Paraquat dichloride hydrate (PQ), diquat dibromide monohydrate, atrazine (ATR), simazine and propazine (all in PENTANAL® analytical standard grade) as well as 1-ethyl-3-(3-dimethylamonopropyl) carbodiimide (EDC) were purchased from Sigma-Aldrich (St. Louis, MO). Anti-atrazine rabbit polyclonal antibody (anti-ATR antibody) and atrazine-BSA conjugate (ATR-BSA) were from United Immunoassay (San Bruno, California), and mouse monoclonal anti-paraquat antibody (anti-PQ antibody) from Selective Antibodies Ltd (Newcastle upon Tyne, UK). Goat anti-rabbit IgG and goat anti-mouse IgG antibodies were purchased from Sigma-Aldrich and Merck-Millipore (Billerica Massachusetts, USA), respectively. The water used throughout the study was doubly distilled.

2.2. Instrumentation

The detection system employed in the present study consists of: a) a visible/near infra-red light source, b) a miniaturized spectrophotometer (Maya 2000 Pro, Ocean Optics) with a resolution of 0.25 nm, and c) a reflection probe (AVANTES Inc., Broomfield, CO) which delivers the incident light to the surface through six multi-mode fibers arranged in the periphery of the probe and collects the reflected light through the central fiber which is connected to the spectrophotometer. Each one of the seven fibers of the reflection probe has a diameter of 400 microns. For the measurements, the chips were assembled with the fluidic compartment manufactured by Jobst Technologies GmbH (Freiburg, Germany). The fluidic is composed of a 2-mm thick PMMA cover with milled fluid inlet and outlet to which a 200-μm thick double side adhesive appropritely cut to form the reaction chamber has been applied (Fig. S1a). The dimensions of the reaction chamber were 12 mm x 2.5 mm x 0.2 mm (LxWxH). After assembly with the fluidic compartment, the chip is placed in the docking station that is mounted on a linearly moving stage with position accuracy of 10 microns (Parker, Charlotte, NC) (Fig. S1b). A miniaturized peristaltic pump (based on the CPP1-150 unit of Jobst Technologies GmbH) was employed for the reagents delivery to the chip. Data aquisition was performed by a custom-made FR-Monitor software that controlled both the linear stage and the optical set-up. An integration time of 15 ms was set for the spectrometer and the reflectance spectrum was recorded every second. Using a step of 0.5 mm, a length of 4 mm was scanned across the chip long axis and each scanning cycle lasted 8 s. To monitor bioreactions taking place on the sensor, the absolute reflectance spectrum [R(λ)] was calculated using the following equation:

$$R(\lambda)=(S(\lambda)-D(\lambda))/(REF(\lambda)-D(\lambda)) \times 100$$

where, D(λ) is the dark spectrum received with the light source turned-off, REF(λ) is the reference spectrum, and S(λ) is reflectance spectrum recorded every second from the sensing surface. In Fig. S2a, a dark, a reference, and a characteristic reflectance spectrum are provided.

The absolute reflectance spectrum is then fitted in the 450-560 nm spectral range using the Levenberg-Marquart algorithm for a layer stack consisted of water/biomolecular layer/SiO_2/Si and assuming a refractive index value of 1.45 for the biomolecular layer [57]. The red spectral shift of the reflectance spectrum recorded in the course of the biomolecular reaction (Fig. S2b) is interpreted as thickness increase and it is attributed to "effective biomolecular layer thickness" and not the absolute thickness of biomolecular layer formed on the sensor surface. Processing of the spectrum and transformation of the spectral shift to "effective biomolecular layer thickness" is performed in real-time by the dedicated software provided with the sensing system.

2.3. Calibrator and water samples preparation

A stock solution with concentration of 1 mg/mL was prepared for each pesticide (PQ, ATR) in methanol and stored at -20 ^{o}C. From this solution, calibrators with concentrations ranging from 0.05 to 5.0 ng/mL were prepared for each pesticide in 0.05 M phosphate buffer, pH 7.4, containing 0.9% (w/v) NaCl and 0.2% (w/v) BSA (assay buffer) as well as in bottled table water. Samples fortified with known concentrations of the two pesticides were prepared in bottled table water as well as in tap water.

2.4. Preparation of PQ-BSA conjugates

The paraquat molecule (Fig. 2a) does not have a reactive group appropriate for direct coupling to protein molecules, therefore two derivatives, one with bromovaleric ester (Fig. 2b) and the second one with cyanuric chloride (Fig. 2c) were synthesized following slightly modified literature methods [17, 58]. The detailed protocols for the preparation of these derivatives as well as their characterization by ^{1}H NMR are provided in Supplementary data.

For the preparation of paraquat-BSA conjugate using the paraquat-valeric acid (PQ-VAL) derivative, 1.6 mg of PQ-VAL in 280 µL of 0.1 M MES buffer, pH 4.7, were mixed with 160 µL of a 13 mg/mL BSA solution in the same buffer. To this mixture 100 µL of a 10 mg/ml EDC solution in water were added, and the reaction mixture was incubated for 2 h at room temperature (RT). Afterwards the reaction mixture was extensively dialyzed against 0.1 M $NaHCO_3$, pH 8.5, 0.15 M NaCl, 0.05 mg/mL NaN_3, and stored at 4 ºC.

The conjugation of paraquat-cyanuric chloride (PQ-CN) to BSA was performed by mixing 500 µL of a 2 mg/mL BSA solution in 50 mM carbonate buffer, pH 9.3, with 500 µL of a 1 mg/mL PQ-CN solution prepared in a 3:7 mixture of 50 mM carbonate buffer, pH 9.3, and dimethyl sulfoxide. The reaction mixture was incubated for 2 hours at RT and then, extensively dialyzed against 0.1 M $NaHCO_3$, pH 8.5, 0.15 M NaCl, 0.05 mg/mL NaN_3, and stored at 4 ºC.

2.5. Preparation of the biochip

The immobilization of biomolecules onto the SiO_2 top layer of the chips requires chemical activation with a silane layer. Prior to activation, the chips were cleaned/hydrophilized by O_2 plasma treatment for 30 s in a Reactive Ion Etcher at 10 mTorr. Then, they were immersed in a 2% (v/v) aqueous APTES solution for 20 min, washed with distilled water, dried under a nitrogen stream, cured at 120 ºC for 20 min, and kept at RT in a desiccator for at least 24 h prior to use. The PQ-VAL-BSA and ATR-BSA conjugates were then deposited as two spatially distinct bands on the APTES-modified chips through spotting from solutions prepared in 100 mM carbonate buffer, pH 9.2, using the Bio-Odyssey Calligrapher microarray spotter (Bio-Rad Laboratories, Hercules, CA). Bands covering an area of 1.1x3.6 mm^2 were created by deposition of 10 lines of 35 spots each with a spot-to-spot distance of 100 µm. After spotting, the chips were incubated in controlled humidity (75%) overnight at 4 ºC. Then, they were washed with 10 mM phosphate buffer, pH 7.4, 9 g/L NaCl (washing solution), and immersed

in blocking solution (10 mg/mL BSA in 0.1 M $NaHCO_3$, pH 8.5) for 1 h at RT. After rinsing with washing solution and distilled water the chips were dried under a nitrogen stream and used for the assay. The biofunctionalized chips are mentioned hereinafter as biochips.

2.6. Dual-analyte assay

At first, assay buffer was run over the biochip for 2 min to acquire a stable baseline, then 1:1 volume mixtures of calibrators or water samples with a solution containing the two analyte-specific antibodies (2 μg/mL of anti-ATR antibody and 2 μg/mL of anti-PQ antibody in assay buffer) were passed over the biochip for 7 min with a flow rate of 50 μL/min (total sample volume 350 μL). After that, a solution containing 5 μg/mL of anti-mouse IgG antibody and 5 μg/mL of anti-rabbit IgG antibody in assay buffer were run for 5 min at the same flow rate. Finally, the biochip was regenerated by passing a 0.5% (w/v) SDS solution, pH 1.9, for 2 min, followed by equilibration with assay buffer. According to competitive immunoassay principle followed for the detection of ATR and PQ, the maximum signal is obtained in absence of analyte, i.e., for the zero calibrator; whereas in presence of analyte due to "competition" between the solid-phase immobilized analyte-conugate and the analyte in the calibrator/sample for binding to the free binding sites of the antibody, the signal decreases inversely proportional to the analyte concentration. Thus, the ATR and PQ calibration curves were created by plotting the effective biomolecular layer thickness (signal) obtained for the different calibrators (S_x) as percentage of the zero calibrator signal (maximum signal; S_0) against the respective analyte concentration in the calibrator solutions in linear/log scale.

3. Results and discussion

3.1. Selection of PQ-BSA conjugate

Two different PQ-BSA conjugates were synthesized starting from two different derivatives, the first bearing a valeric acid moiety (PQ-VAL) and the second a cyanuric chloride moiety (PQ-CN). Both derivatives were coupled to BSA through reaction with its reactive ε-amine groups, the first after conversion to active ester (via reaction with EDC) and the second directly [57]. The two conjugates, PQ-VAL-BSA and PQ-CN-BSA, were compared with respect to zero calibrator signal and the assay sensitivity (percent inhibition in presence of analyte). In Fig. 3a, the zero calibrator values obtained for a range of anti-PQ antibody concentrations versus the concentration of the conjugate used for coating is presented for both conjugates. As shown, the conjugate prepared using the cyanuric chloride derivative (PQ-CN-BSA) provided lower zero calibrator signal values for all the anti-PQ antibody concentrations employed compared to the conjugate prepared with the valeric acid derivative (PQ-VAL-BSA). This is probably the result of the higher molar ratio of PQ per BSA achieved using the valeric acid derivative rather than the cyanuric chloride one. Thus, in order to achieve similar zero calibrator values higher concentrations of PQ-CN-BSA are required for the same anti-PQ antibody concentration as compared to the PQ-VAL-BSA conjugate. In this case, as shown in Fig. 3b, the percent inhibition values obtained for different PQ calibrators from biochips coated with concentrations of the two conjugates that provided similar zero calibrator values, was marginally higher when the PQ-VAL-BSA conjugate was employed. Thus, this conjugate was selected for further experimentation.

3.2. Assay optimization

The optimization of the assays for the two pesticides was performed separately using biochips with a single immunoreactive band. The two most important parameters for a competitive immunoassay are the concentration of analyte-protein conjugate used for coating and the concentration of analyte-specific antibody, since they define the absolute signal but also the

assay sensitivity. Thus, the criteria for the optimization of these two parameters are the maximum signal achieved in absence of analyte, i.e., the zero calibrator signal, and the percent signal drop obtained in presence of calibrators which defines the assay sensitivity. Since increase of the conjugate and the antibody concentration usually increases the zero calibrator signal while at the same time decreases the assay sensitivity, conditions that counterbalance these two effects are selected. Regarding the PQ assay, as shown in Fig. 3a, maximum plateau zero calibrator signal values were obtained when concentrations of PQ-VAL-BSA conjugate equal to 100 μg/mL for antibody concentrations ranging from 1.0 to 4.0 μg/mL, whereas a conjugate concentration of 50 μg/mL provided values that corresponded to more than 90% of the maximum plateau ones. Thus, in order to use the minimum possible conjugate concentration, a 50 μg/mL PQ-VAL-BSA conjugate concentration was selected for further experimentation since it provided slightly improved detection sensitivity. Biochips coated with a 50 μg/mL of PQ-VAL-BSA conjugate provided plateau zero calibrator signal values for anti-PQ antibody concentrations equal to or higher than 4 μg/mL. Nonetheless, as shown in Fig. S3, the assay sensitivity was greatly improved when a 2 μg/mL antibody solution was used compared to higher concentrations, and thus, this concentration was adopted in the final protocol.

For the ATR assay, the zero calibrator signals obtained using different concentrations of ATR-BSA conjugate in the coating solution in combination with different anti-ATR antibody concentrations are provided in Fig. 4a. As shown, maximum plateau values were obtained when ATR-BSA conjugate concentrations higher than 10 μg/mL were used for coating with all the anti-ATR antibody concentrations tested, and thus this concentration was selected. The optimum anti-ATR antibody concentration was selected based on both the zero calibrator signal and the assay sensitivity. As shown in Fig. 4b, the assay sensitivity was marginally improved when the anti-ATR antibody concentration was reduced from 2 to 1 μg/mL.

Therefore, in order to achieve adequate zero calibrator signal and assay sensitivity a 2 μg/mL anti-ATR antibody concentration was adopted in the final protocol.

Another parameter optimized was the duration of the two immunoreaction steps. As shown in Fig. S4a, for the PQ assay the signal was continuously increased during the primary immunoreaction (i.e., the reaction of the pesticide-specific antibody with the immobilized conjugate) even after 2 h. Nonetheless, the percent signal drop (inhibition) achieved in presence of PQ was reduced as the primary immunoreaction time was increased with the highest percent inhibition achieved for 7-min reaction with the anti-PQ antibody. Regarding ATR, the primary immunoreaction reached maximum plateau values after 2 h, with more than 70% of the signal to be obtained after only 7-min (Fig S4b). This reaction time corresponded also to the highest percent inhibition in presence of analyte. Concerning the secondary immunoreactions, maximum plateau values were achieved for both antibodies after 30 min (Fig S4c & 4d). Nonetheless, more than 50% of the maximum signal was obtained for 5-min reaction, providing for both assays zero calibrator signals higher than 1 nm. Thus, a 7-min reaction with the pesticide-specific antibody followed by 5-min reaction with the secondary antibodies was adopted in the final protocol so as to keep the total assay duration as short as possible.

3.3. Specificity and cross reactivity of specific antibodies

The specificity of the anti-ATR and anti-PQ antibody towards the other analyte in the panel was first investigated. For this purpose, each of the antibodies was run separately over biochips with dual-analyte bands. As shown in Fig. 5, response was obtained from each pesticide-conjugate band only when the respective specific antibody was run over the chip. The response obtained from the band corresponding to the second analyte in the panel was negligible and

could not be distinguished from the response obtained from the blocked area between the two bands that corresponds to non-specific binding signal. The specificity of each antibody response towards the two analytes of the panel is also supported by the fact that the calibration curves obtained for the two analytes with the dual-analyte sensor were identical to those received from the respective single analyte chips (see Fig. S5 of Supplementary data).

In addition to the selectivity of the antibodies towards the two analytes of the panel, the cross-reactivity with compounds of high structural similarity with ATR or PQ was evaluated. In particular, the cross-reactivity of anti-ATR antibody against two other compounds of the triazine class herbicides, namely simazine and propazine, was determined, whereas the anti-PQ antibody was tested against monoquat and diquat; monoquat is a metabolite of PQ while diquat is also an herbicide used worldwide. The chemical structures of the compounds checked as cross-reactants are presented in Table 2. To determine cross-reactivity, calibrators of each one of the potential cross-reactants were prepared and run as single-analyte assays using biochips functionalized either with ATR-BSA or PQ-VAL-BSA conjugate and using the anti-ATR or anti-PQ antibody, respectively. Percent cross-reactivity (%CR) was calculated by the following formula: %CR = (IC_{50} target analyte/IC_{50} cross-reactant)x100, where IC_{50} target analyte is the concentration of ATR or PQ, respectively, providing 50% inhibition of the zero calibrator signal and IC_{50} cross-reactant is the concentration of possible cross-reactant resulting to 50% inhibition of the respective curve (see Fig. S6 of Supplementary data). As shown in Table 1, simazine and propazine exhibited cross-reactivity values of 25.0 and 16.7%, respectively, indicating that the rabbit polyclonal antibody against ATR employed in the current study recognized to a great extent the other two triazines. Nonetheless, one can consider this cross-reactivity as an advantage, since both simazine and propazine are herbicides that exhibit endocrine disruptive properties and therefore their use has been banned within EU.

Thus, although a positive sample might need to be further analysed by an HPLC-based method to identify the exact compounds in the sample, the proposed sensor can serve as a screening tool for the rapid analysis of numerous samples at significantly lower cost than the HPLC-based methods. On the other hand, the mouse monoclonal antibody against PQ was highly specific since negligible percent inhibition was observed for monoquat and diquat concentrations up to 1000 ng/mL (Fig. S6b).

3.4. Analytical characteristics of the dual-analyte assays

The effect of water matrix on the assays was assessed to define the optimum medium for the preparation of calibrators as well as the necessity for water sample pre-treatment. For this purpose, calibrators were prepared in bottled and in tap water and the calibration curves obtained were compared to the one received using calibrators prepared in assay buffer. As it can be concluded from Fig. S7, the three calibration curves were identical, thus allowing to directly analyze drinking water samples without any treatment.

Typical calibration curves for PQ and ATR obtained with the dual-analyte sensor are provided in Fig. 6. The assays limit of detection (LOD) was calculated as the concentration corresponding to mean zero calibrator signal obtained from 10 assay runs minus 3 standard deviations (SD), and was 50 and 40 pg/mL for ATR and PQ, respectively. The limit of quantification (LOQ) was determined as the concentration corresponding to mean zero calibrator signal obtained from 10 assay runs minus 6 SD, and was 100 and 80 pg/mL for PQ and ATR, respectively, while the assays working ranges were up to 2.5 and 5.0 ng/mL, respectively.

The assay repeatability was determined using three control samples prepared in bottled water spiked with three different concentration levels of the two pesticides. The intra-assay coefficient of variation (CV) was determined by running 3 replicates of each control in the same day while the inter-assay CV was determined by duplicate measurements performed in 5 days over a period of one month. For both assays, the intra- and inter-assay CV values were less than 10% and 12%, respectively, for the three control samples. The assays accuracy was evaluated through recovery experiments. For this purpose, tap and two bottled water samples were spiked with 3 different concentrations of each one of the pesticides (0.2, 0.4 and 1.2 ng/mL). All samples were analyzed in triplicate both prior to and after the addition of pesticides and the percent recovery values were calculated according to the equation:

%Recovery = [Amount determined/Amount added] × 100

As shown in Table 2, the recovery values determined ranged between 90.0 and 110% for PQ and between 92.0 and 105% for ATR, indicating the good accuracy of the immunosensor developed.

3.5. Regeneration capability and re-use of the biosensor

The ability to regenerate the biochip is a significant asset since its re-use could reduce considerably the analysis cost. The following solutions have been evaluated as possible regeneration reagents: a commercially available IgG elution buffer for immunoaffinity columns, a 0.1 M glycine-HCl buffer, pH 2.5, a 50 mM NaOH, a 100 mM HCl, and a 0.5% (w/v) SDS adjusted to pH 1.9 with HCL solution. Each regeneration buffer was run for 3 min over the chip after the assay, followed by reaction with the respective secondary antibody to determine the percent ratio of anti-pesticide specific antibody that has not been removed. As shown in Fig. 7a, the solution that removed more efficiently the bound antibodies was 0.5%

(w/v) SDS, pH 1.9 (less than 5% of bound antibody molecules remain). In addition, the percentage of the signal obtained when running the secondary antibodies after regeneration remained stable for several repetitive assay/regeneration cycles. Thus, this solution was selected for regeneration and the duration of this step was further optimized. It was found that the minimum time which provided efficient removal of bound antibodies from the pesticide-conjugates immobilized onto the biochip was 2 min.

Using the selected regeneration solution, the stability of the biochips towards regeneration was assessed through repetitive assay/regeneration cycles. As shown in Fig. 7b, at least 20 assay/regeneration cycles could be performed without affecting the signal obtained for the zero calibrator since all values were within the mean value of 20 determinations ± 2SD limits.

3.6. Comparison with optical label-free literature methods

The necessity for pesticides determination at the point-of-need has motivated the implementation of several biosensing principles for the development of appropriate tools. In Table 3, the LODs, working ranges, assays duration and sample type of optical sensors that have been reported in the literature for the determination of either ATR or PQ are provided. Regarding ATR, the earliest reports date back to 1993, and include sensors based on surface plasmon resonance (SPR) [37-43], reflectance interference spectroscopy (RIfS) [44], Mach-Zehnder interferometers [45], resonant mirrors [47], waveguides [48] and reflection-absorption IR spectroscopy (RAIRS) [49]. The SPR sensors employ either antibodies [38, 40, 41], a plastoquinone binding protein [39], or molecularly imprinted polymers (MIPs) [42, 43] as recognition molecules. Antibodies and MIPs are in general more specific and provide for lower LODs which are comparable to that achieved with the proposed sensor. The only exception is an SPR sensor with a MIP as capture molecule that claims an LOD of 2 fg/mL [43], calculated, nonetheless, based on the instrument signal resolution rather than detection in actual samples.

Regarding the other types of sensors so far implemented for ATR detection [44, 45, 47-49], they are all based on competitive immunoassay format and demonstrate LODs that are 2 to 6-times higher than that achieved with the proposed dual-analyte immunosensor.

The sensors reported for PQ can be divided into two categories; immunosensors and spectroscopic sensors based on Surface Enhanced Raman Scattering (SERS). From the immunosensors, two reports [21, 22] are optical immunosensors that follow a competitive immunoassay format employing fluorescently labelled antibodies for the detection. The first immunosensor [21] achieves an LOD in drinking water that is 4-times lower than that of the proposed sensor for the same assay duration when the calibrators are prepared in ultra-pure water, while it has a similar LOD when calibrators are prepared in river water. The second [22] has a comparable LOD for an assay time of 30 min; nonetheless, four pesticides are determined simultaneously. The third immunosensor reported for the determination of PQ employed a commercially available SPR instrument to explore a strategy for signal amplification through the implementation of a PQ dimer as bridge between different antibody molecules so as to increase the amount of anti-PQ antibodies immobilized onto the sensor surface [23]. The authors do not mention the LOD achieved and the lowest PQ concentration they use is 51 ng/mL. The main advantage of this sensor is that the assay duration is only 1 min. Regarding the three reports [24-26] for PQ determination by SERS, they demonstrated LODs that were 12 to 62-times higher than that of the proposed method, and therefore they are more suitable for determination of PQ in agricultural products for which the maximum allowable limits are much higher than those for drinking water (0.05 to 500 g/kg). Moreover, the time required for the recording and analysis of the spectra is not specified, while the of-line processing of the data means that, for the time being, no real-time monitoring is possible. In conclusion, the proposed sensor, that is the first sensor for simultaneous determination of ATR and PQ, demonstrates analytical sensitivity that is comparable or higher than that provided by other

literature sensors and adequate for the determination of the two pesticides in drinking water samples.

Conclusions

A sensor for the simultaneous determination of paraquat and ATR in drinking water samples was developed. The sensor was based on the WLRS principle which allowed for the label-free and real-time monitoring of immunochemical interactions. The assays developed were highly sensitive, rapid and accurate. Thus, taking into account the excellent analytical performance and short analysis time along with the small sensor size it seems that it can be evolved in a portable device for determination of pesticides at the point-of-need.

References

[1] E. Petryayeva, W. R. Algar, Toward point-of-care diagnostics with consumer electronic devices: the expanding role of nanoparticles, RSC Adv. 5 (2015) 22256-22282.

[2] A. Sassolas, B. Prieto-Simón, J.-L. Marty, Biosensors for Pesticide Detection: New Trends, Am. J. Anal. Chem. 3 (2012) 210-232.

[3] S.Q. Liu, Z.Z. Zheng, X.Y. Li, Advances in pesticide biosensors: current status, challenges, and future perspectives, Anal. Bioanal. Chem. 405 (2013) 63-90.

[4] N. Verma, A. Bhardwaj, Biosensor Technology for Pesticides-A review, Appl. Biochem. Biotechnol. 175 (2015) 3093-3119.

[5] F.P. Carvalho, Pesticides, environment, and food safety, Food Energ. Sec. 6 (2017) 48-60.

[6] K.H. Kim, E. Kabir, S.A. Jahan, Exposure to pesticides and the associated human health effects, Sci. Total Environ. 575 (2017) 525-535.

[7] J.C.G. Sousa, A.R. Ribeiro, M.O. Barbosa, M.F.R. Pereira, A.M.T. Silva, A review on environmental monitoring of water organic pollutants identified by EU guidelines, J. Hazard. Mater. 344 (2018) 146-162.

[8] S. Li, P.A. Crooks, X. Wei X, J. de Leon, Toxicity of dipyridyl compounds and related compounds. Crit. Rev. Toxicol. 34 (2004) 447-60.

[9] A. Moretto, C. Colosio, Biochemical and toxicological evidence of neurological effects of pesticides: The example of Parkinson's disease, Neurotoxicol. 32 (2011) 383-391.

[10] R. Franco, S. Li, H. Rodriguez-Rocha, M. Burns, M.I. Panayiotidis, Molecular mechanisms of pesticide-induced neurotoxicity: Relevance to Parkinson's disease, Chem. Biol. Interact. 188 (2010) 289-300.

[11] D. Kolberg, D. Mack, M. Anastassiades, M.T. Hetmanski, R.J. Fussell, T. Meijer, H.G. Mol, Development and independent laboratory validation of a simple method for the

determination of paraquat and diquat in potato, cereals and pulses, Anal. Bioanal. Chem. 404 (2012) 2465-74.

[12] B. Sun, Y. Chen, A simple and rapid method for detection of paraquat in human plasma by high-performance liquid chromatography, Int. J. Clin. Exp. Med. 8 (2015) 17067-17071.

[13] T. Zou, P. He, J. Cao, Z. Li, Determination of paraquat in vegetables using HPLC-MS-MS. J. Chromatogr. Sci. 53 (2015) 204-209.

[14] W. Zhang, Y. Su, J. Shi, M. Zhang, B. Wu, S. Chen, S. Hu, Z. Rao, J. Zheng, Reversed-phase high performance liquid chromatography method for the determination of paraquat in whole blood, Anal. Method 6 (2014) 6560–6564.

[15] I. R. Pizzutti, G.M.E. Vela, A. de Kok, J.M. Scholten, J.V. Dias, C.D. Cardoso, G. Concenço, R. Vivian, Determination of paraquat and diquat: LC-MS method optimization and validation, Food Chem. 209 (2016) 248-255.

[16] M.R. Bowles, D.W. Eyles, E.C.G.M. Hampson, S.M. Pond, Quantitation of Paraquat in Biological Samples by Radioimmunoassay Using a Monoclonal Antibody, Fund. Appl. Toxicol. 19 (1992) 375-379.

[17] R. Garcia-Febrero, , J.-P. Salvador, F. Sanchez-Baeza, M.-P. Marco, Rapid method based on immunoassay for determination of paraquat residues in wheat, barley and potato, Food Control 41 (2014) 193-201.

[18] E. Valera, R. García-Febrero, I. Pividori, F. Sánchez-Baeza, M.-P. Marco, Coulombimetric immunosensor for paraquat based on electrochemical nanoprobes, Sensor Actuator B 194 (2014) 353-360.

[19] H. El Harmoudi, M. Achak, A. Farahi, S. Lahrich, L. El Gaini, M. Abdennouri, A. Bouzidi, M.Bakasse, M.A. El Mhammedi, Sensitive determination of paraquat by square wave anodic stripping voltammetry with chitin modified carbon paste electrode, Talanta115 (2013) 172-177.

[20] L.C.S. de Figueiredo-Filho, M. Baccarin, B.C. Janegitz, O. Fatibello-Filho, A disposable and inexpensive bismuth film minisensor for avoltammetric determination of diquat and paraquat pesticides innatural water samples, Sensor Actuator B 240 (2017) 749-756.

[21] E. Mallat, C. Barzen, R. Abuknesha, G. Gauglitz, D. Barceló, Fast determination of paraquat residues in water by an optical immunosensor and validation using capillary electrophoresis-ultraviolet detection, Anal. Chim. Acta 427 (2001) 165-171.

[22] C. Mastichiadis, S.E. Kakabakos, I. Christofidis, M.A. Koupparis, C. Willetts, K. Misiakos, Simultaneous determination of pesticides using a four-band disposable optical capillary immunosensor, Anal. Chem. 74 (2002) 6064-6072.

[23] H. Yamaguchi, A. Harada, Supramolecular formation of antibodies with viologen dimers: Utilization for amplification of methyl viologen detection signals in surface plasmon resonance sensor, Biomacromolecules 3 (2002) 1163-1169.

[24] R. Gao, N. Choi, S.-I. Chang, S.H. Kang, J.M. Song, S.I. Cho, D.W. Lim, J. Choo, Highly sensitive trace analysis of paraquat using a surface-enhanced Raman scattering microdroplet sensor, Anal. Chim. Acta 681 (2010) 87-91.

[25] H. Fang, X. Zhang, S. J. Zhang, L. Liu, Y.M. Zhao, H.J. Xua, Ultrasensitive and quantitative detection of paraquat on fruits skinsvia surface-enhanced Raman spectroscopy, Sensor Actuator B 213 (2015) 452-456.

[26] C. Wang, X. Wu, P. Dong, J. Chen, R. Xiao, Hotspots engineering by grafting Au@Ag core-shell nanoparticles on the Au film over slightly etched nanoparticles substrate for on-site paraquat sensing, Biosens. Bioelectron. 86 (2016) 944-950.

[27] N.D. Jablonowski, S. Koppchen, D. Hofmann, A. Schaffer, P. Burauel, Persistence of 14C-labeled atrazine and its residues in a field lysimeter soil after 22 years, Environ. Pollut. 157 (2009) 2126-2131.

[28] S.K. Golfinopoulos, A.D. Nikolaou, N.S. Thomaidis, A.M. Kotrikla, M.C. Vagi, A.S. Petsas, D.F. Lekkas, T.D. Lekkas, Determination of the priority substances regulated by 2000/60/EC and 2008/105/EC Directives in the surface waters supplying water treatment plants of Athens, Greece, J. Environ. Sci. Health A 52 (2017) 378-384.

[29] L.A. Cragin, J.S. Kesner, A.M. Bachand, D. Boyd Barr, J.W. Meadows, E.F. Krieg, J.S. Reif, Menstrual cycle characteristics and reproductive hormone levels in women exposed to atrazine in drinking water, Environ. Res. 111 (2011) 1293-1301.

[30] M.M. Sanagi, H.H. Abbas, W.A.W. Ibrahim, H.Y. Aboul-Enien, Dispersive liquid-liquid microextraction method based on solidification of floating organic droplet for the determination of triazine herbicides in water and sugarcane samples, Food Chem. 133 (2012) 557-562.

[31] M. Zarejousheghani, P. Fiedler, M. Moder, H. Borsdorf, Selective mixed-bed solid phase extraction of atrazine herbicide from environmental water samples using molecularly imprinted polymer, Talanta 129 (2014) 132-138.

[32] F.N. Andrade, C.E. Domingues Nazario, A.J. Santos Neto, F.M. Lancas, Development of an on-line molecularly imprinted solid phase extraction by liquid chromatography-mass spectrometry for triazine analysis in corn samples, Anal. Method 8 (2016) 1181-1186.

[33] N. Sai, W. Sun, Y. Wu, Z. Sun, G. Yu, G. Huang, A highly sensitive immunoassay for atrazine based on covalently linking the small molecule hapten to a urea-glutaraldehyde network on a polystyrene surface. Int. Immunopharmacol. 40 (2016) 480-486.

[34] H. Barchanska, E. Jodo, R.G. Price, I. Baranowska, R. Abuknesha, Monitoring of atrazine in milk using a rapid tube-based ELISA and validation with HPLC, Chemosphere 87 (2012) 1330-1334.

[35] C. Tortolini, P. Bollella, R. Antiochia, G. Favero, F. Mazzei, Inhibition-based biosensor for atrazine detection, Sensor Actuator B 224 (2016) 552-558.

[36] E. Valera, J. Ramon-Azcov, F.-J. Sanchez, M.-P. Marco, A. Rodrıguez, Conductimetric immunosensor for atrazine detection based on antibodies labelled with gold nanoparticles. Sensor Actuator B 134 (2008) 95-103.

[37] N. Belkhamssa, C.I.L. Justino, P.S.M. Santos, S. Cardoso, I. Lopes, A.C. Duarte, T. Rocha-Santos, M. Ksibi, Label-free disposable immunosensor for detection of atrazine. Talanta 146 (2016) 430-434.

[38] M. Minunni, M. Mascini (1993) Detection of pesticide in drinking water using real-time biospecific interaction analysis (BIA), Anal. Lett. 26 (1993) 1441-1460.

[39] V.I. Chegel, Y.M. Shirshov, E.V. Piletskaya, S.A. Piletsky, Surface plasmon resonance sensor for pesticide detection Sensor Actuator B 48 (1998) 456-460.

[40] M. Shimomura, Y. Nomura, W. Zhang, M. Sakino, K.-H, Lee, K. Ikebukuro, I. Karube, Simple and rapid detection method using surface plasmon resonance for dioxins, polychlorinated biphenyls and atrazine, Anal. Chim. Acta 434 (2001) 223-230.

[41] M. Farré, E. Martínez, J. Ramón, A. Navarra, J. Radjenovic, E. Mauriz, L. Lechuga, M.P. Marco, D. Barceló, Part per trillion determination of atrazine in natural water samples by a surface plasmon resonance immunosensor, Anal. Bioanal. Chem. 388 (2007) 207-214.

[42] H. Agrawal, A.M. Shrivastav, B.D. Gupta, Surface plasmon resonance based optical fiber sensor for atrazine detection using molecular imprinting technique, Sensor Actuator B 227 (2016) 204-211.

[43] E. Yılmaz, E. Özgür, N. Bereli, D. Türkmen, A. Denizli, Plastic antibody based surface plasmon resonance nanosensors for selective atrazine detection, Mater. Sci. Eng. C 73 (2017) 603-610.

[44] A. Brecht, J. Piehler, G. Lang, G. Gauglitz, A direct optical immunosensor for atrazine detection, Anal. Chim. Acta 311 (1995) 289-299.

[45] E.F. Schipper, A.J.H. Bergevoet, R.P.H. Kooyman, J. Greve, New detection method for atrazine pesticides with the optical waveguide Mach-Zehnder immunosensor, Anal. Chim. Acta 341 (1997) 171-176.

[46] E. F. Schipper, S. Rauchalles, R. P. H. Kooyman, B. Hock, J. Greve, The waveguide Mach Zender interferometer as atrazine sensor, Anal. Chem. 70 (1998) 1192-1197.

[47] P. Skladal, A. Deng, V. Kolar, Resonant mirror-based optical immunosensor: application for the measurement of atrazine in soil, Anal. Chim. Acta 399 (1999) 29-36.

[48] C.M. Cummins, M.E. Koivunen, A. Stephanian, S.J. Gee, B.D. Hammock, I.M. Kennedy, Application of europium(III) chelate-dyed nanoparticle labels in a competitive atrazine fluoroimmunoassay on an ITO waveguide, Biosens. Bioelectron. 21 (2006) 1077-1085.

[49] M. Salmain, N. Fischer-Durand, C.-M. Pradier, Infrared optical immunosensor: Application to the measurement of the herbicide atrazine, Anal. Biochem. 373 (2008) 61-70.

[50] G. Gauglitz, Direct optical detection in bioanalysis: An update. Anal. Bioanal. Chem. 398 (2010) 398, 2363-2372.

[51] P.S. Petrou, D. Ricklin, M. Zavali, I. Raptis, S.E. Kakabakos, K. Misiakos, J.D. Lambris, Real-time label-free detection of complement activation products in human serum by white light reflectance spectroscopy, Biosens Bioelectron. 24 (2009) 3359-3364.

[52] H. Ouyang, L.A. DeLouise, B.L. Miller, P.M. Fauchet, Label-free quantitative detection of protein using macroporous silicon photonic bandgap biosensors, Anal. Chem. 79 (2007) 1502-1506.

[53] G. Gaur, D.S. Koktysh, S.M. Weiss, Immobilization of quantum dots in nanostructured porous silicon films: Characterizations and signal amplification for dual-mode optical biosensing, Adv. Funct. Mater. 23 (2013) 3604-3614.

[54] R. Liu, W. Li, T. Cai, Y. Deng, Z. Ding, Y. Liu, X. Zhu, X. Wang, J. Liu, B. Liang, T. Zheng, J. Li, TiO_2 Nano-layer enhanced fluorescence for simultaneous multiplex mycotoxin detection by aptamer microarrays on porous silicon surface, ACS Appl. Mater. Interf. 10 (2018) 14447-14453.

[55] G. Koukouvinos, P. Petrou, K. Misiakos, D. Drygiannakis, I. Raptis, G. Stefanitsis, S. Martini, D. Nikita, D. Goustouridis, I. Moser, G. Jobst, S. Kakabakos, Biosens. Bioelectron. 84 (2016) 89-96.

[56] G. Koukouvinos, Z. Tsialla, P.S. Petrou, K. Misiakos, D. Goustouridis, A. Ucles Moreno, A.R. Fernandez-Alba, I. Raptis, S.E. Kakabakos, Fast simultaneous detection of three pesticides by a White Light Reflectance Spectroscopy sensing platform, Sensor Actuator B 238 (2017) 1214-1223.

[57] J. Voros, The density and refractive index of adsorbing protein layers, Biophys. J. 87 (2004) 553-561.

[58] R.A. Abuknesha, C. Luk, Paraquat enzyme-immunoassays in biological samples: assessment of the effects of hapten-protein bridge structures on assay sensitivity. Analyst 130 (2005) 956-963.

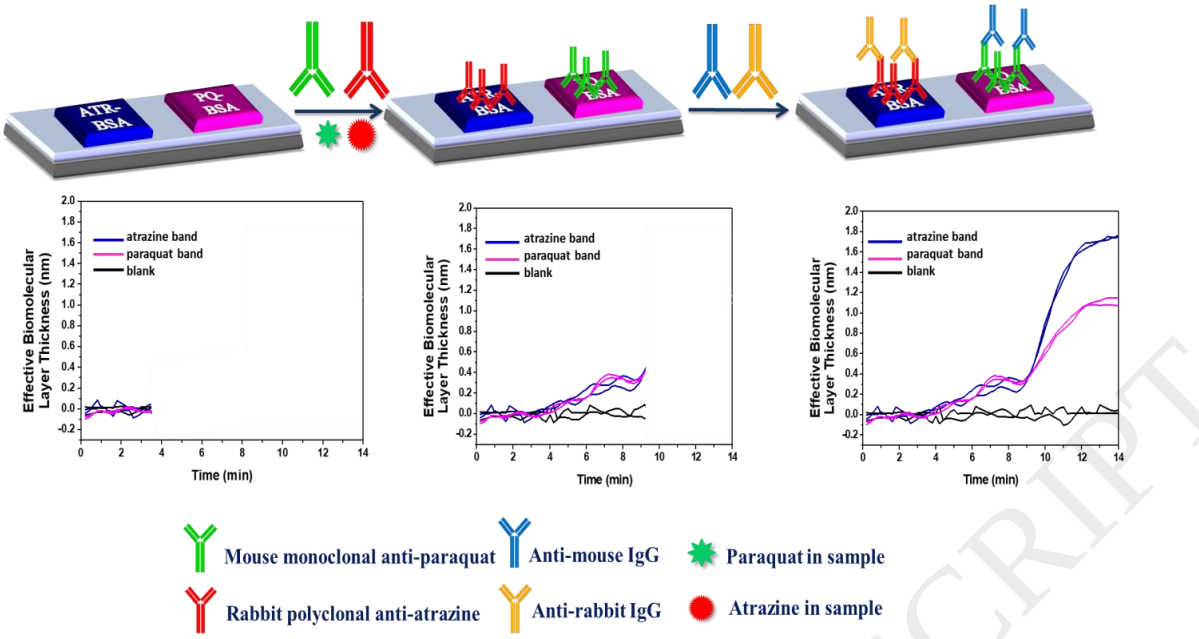

Fig. 1. (top) Schematic of the dual-analyte biochip and the competitive assay format followed for the simultaneous determination of atrazine and paraquat. (bottom) Indicative biomolecular adlayer thickness change during the different steps of the dual-analyte assay depicted at the top part of the figure.

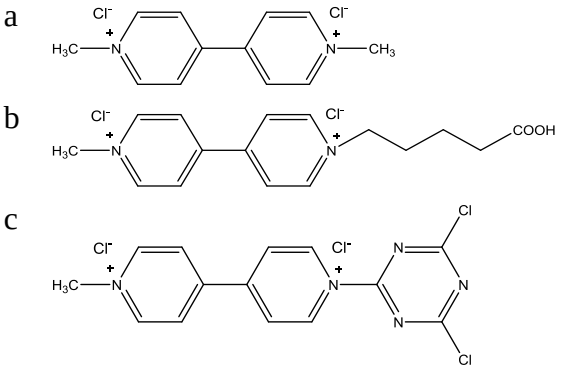

Fig. 2. Molecular structures of (a) paraquat, (b) paraquat-valeric acid, and (c) paraquat-cyanuric chloride derivative.

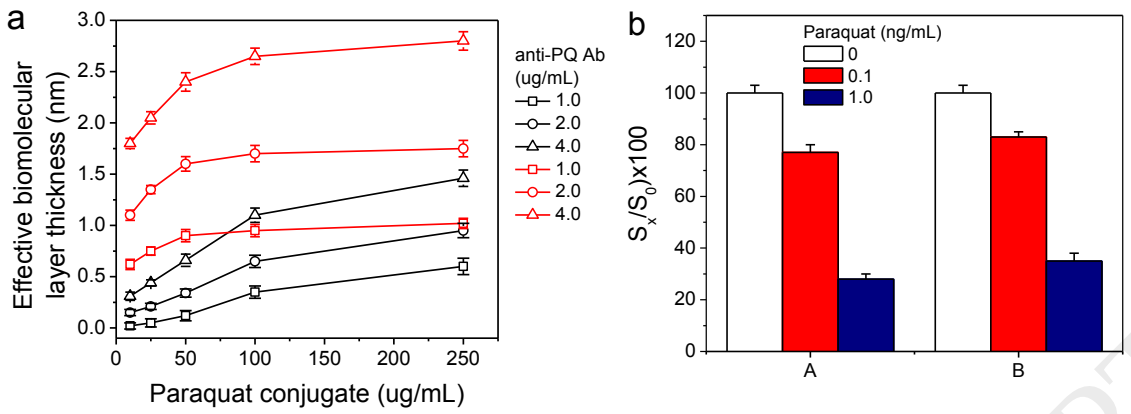

Fig. 3. (a) Effect of PQ-CN-BSA (black lines) and PQ-VAL-BSA (red lines) conjugate concentration used for spotting on the zero calibrator signal obtained using 1.0 (squares), 2.0 (circles) or 4.0 μg/mL (triangles) solution of anti-PQ antibody. (b) Percent inhibition values corresponding to calibrators containing 0.1 (red columns) or 1.0 ng/mL PQ (blue columns) with respect to zero calibrator (white columns) obtained from chips coated with 25 μg/mL of PQ-VAL-BSA (column set A) or 250 μg/mL of PQ-CN-BSA (column set B) when assayed using a 2 μg/mL anti-PQ antibody solution. In all cases, the anti-PQ antibody solution was run for 10 min followed by 5-min reaction with a 5 μg/mL anti-mouse IgG antibody solution. Each point is the mean value of 3 measurements ± SD.

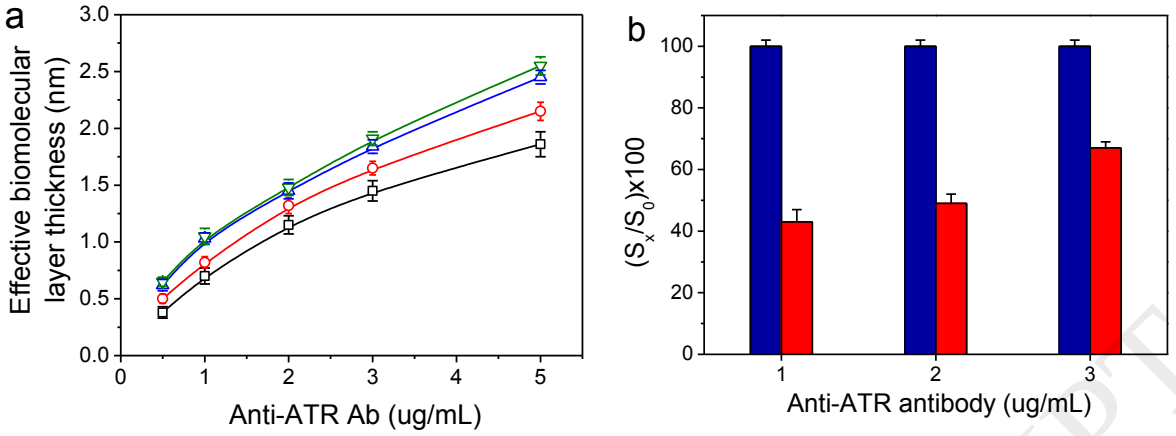

Fig. 4. (a) Effect of anti-ATR antibody concentration on the effective biomolecular layer thickness (zero calibrator signal) obtained from chips coated with 10 (squares), 25 (circles), 50 (up triangles), and 100 μg/mL (down triangles), respectively, of ATR-BSA conjugate. (b) Percent signal corresponding to zero ATR calibrator (blue column) and a calibrator containing 0.25 ng/mL ATR (red columns) obtained from a biochip coated with 10 μg/mL ATR-BSA conjugate versus the anti-ATR antibody concentration. In all cases, the anti-ATR antibody solution was run for 10 min followed by 5-min reaction with a 5 μg/mL anti-rabbit IgG solution. Each point is the mean value of 3 measurements ± SD.

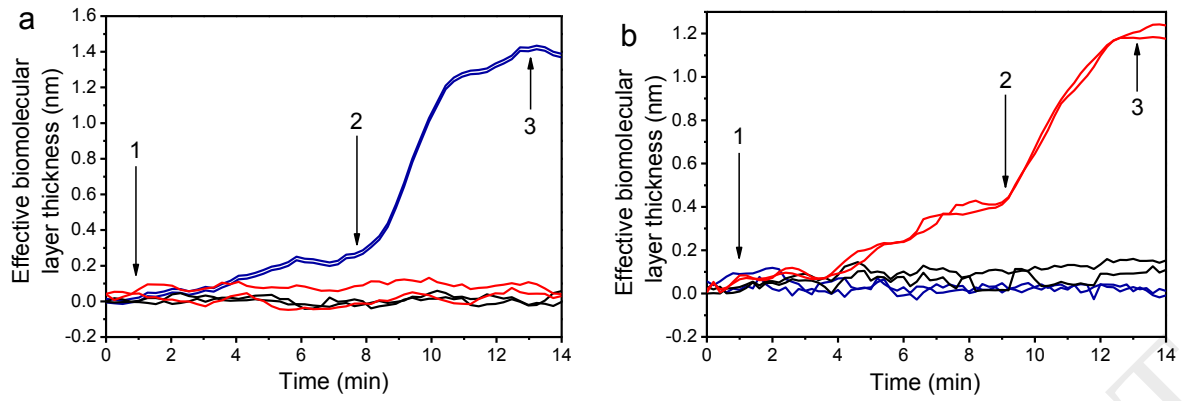

Fig. 5. (a) Real-time sensor responses obtained from a dual-analyte chip upon running (a) the anti-ATR antibody (arrow 1 to 2) followed by the anti-rabbit IgG antibody (arrow 2 to 3), and (b) the anti-PQ antibody (arrow 1 to 2) followed by the anti-mouse IgG antibody (arrow 2 to 3). Blue lines correspond to signal obtained from the ATR-BSA conjugate band, red lines from the PQ-VAL-BSA conjugate band and black lines from the blocked area between the two bands.

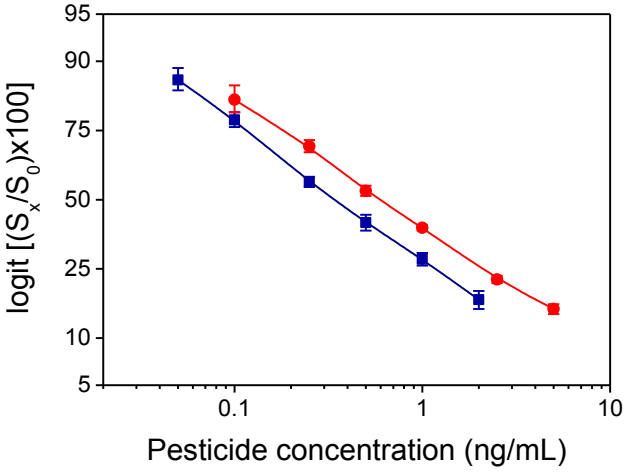

Fig. 6. Typical calibration curves for PQ (blue curve) and ATR (red curve) obtained with the dual-analyte WLRS sensor. Each point is the mean value of 3 replicates ± SD.

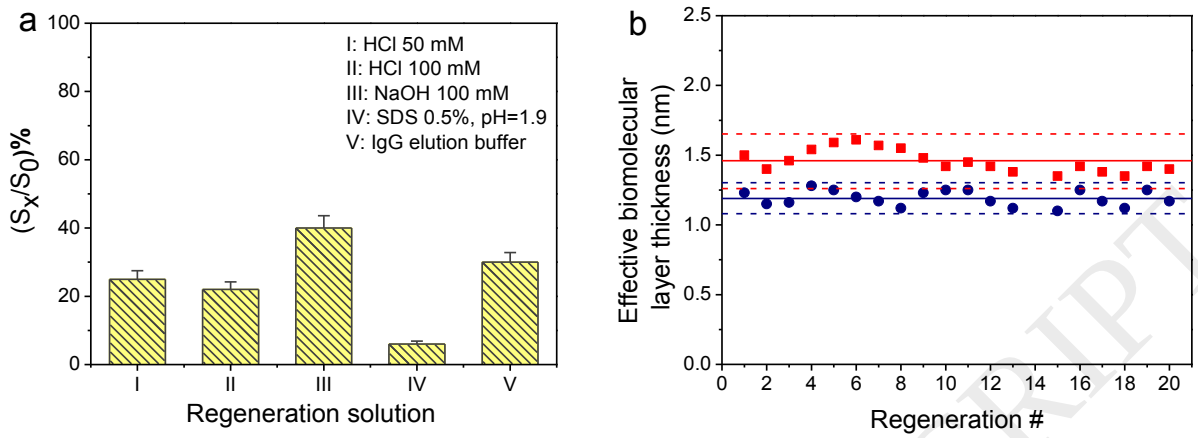

Fig. 7. (a) Percent signal obtained from a chip modified with the ATR-BSA conjugate when running the anti-rabbit IgG antibody after regeneration with respect to the zero calibrator signal. The regeneration solutions tested were: 50 mM HCl (column I), 100 mM HCl (column II), 100 mM NaOH (column III), 0.5% (w/v) SDS, pH 1.9 (column IV), and IgG elution buffer (column V). All regeneration solutions were run over the chip for 3 min. (b) Responses obtained for the zero calibrator from a dual-analyte biochip after 20 cycles of assay and regeneration. Blue circles correspond to PQ and red squares to ATR. Solid lines represent the respective mean value of 20 measurements and dashed lines the ± 2SD limits.

Table 1. Cross reactivity of structurally similar pesticide to atrazine and paraquat assay

Compound	Structure	IC_{50} (ng/mL)	%CR
atrazine	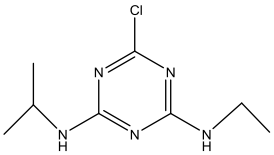	0.60	100
simazine	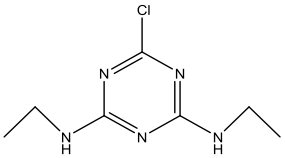	2.4	25.0
propazine	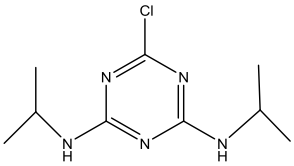	3.6	16.7
paraquat	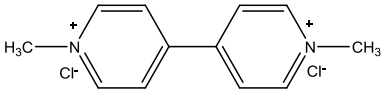	0.36	100
monoquat	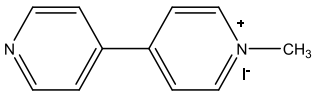	-	0
diquat	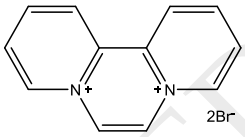	-	0

Table 2. Recovery values determined using tap and drinking water samples spiked with the two pesticides

	Paraquat			**Atrazine**		
Sample	**Amount added (ng/mL)**	**Amount determined (ng/mL)**	**%Recovery**	**Amount added (ng/mL)**	**Amount determined (ng/mL)**	**%Recovery**
Tap Water	0. 10	0.11	110	0.25	0.24	96.0
	0.25	0.24	96.0	1.0	1.0	100
	1.0	0.98	98.0	2.5	2.4	96.0
Bottled Water (Ziria)	0. 10	0.09	90.0	0.25	0.25	100
	0.25	0.27	108	1.0	1.05	105
	1.0	1.05	105	2.5	2.6	104
Bottled Water (Dios)	0. 10	0.11	110	0.25	0.23	92.0
	0.25	0.25	100	1.0	0.95	95.0
	1.0	0.95	95.0	2.5	2.5	100

Table 3. Comparison of analytical characteristics of the developed immunosensor with other optical sensors

Pesticide	Transduction principle	LOD	Dynamic Range	Assay Duration	Application	Ref. #
ATR	**Proposed sensor**	**0.05 ng/mL**	**0.10 - 5.0 ng/mL**	**12 min**	**bottled & tap water**	
	SRP	0.05 ng/mL	0.1 - 1.0 ng/mL	15 min	distilled & tap water	38
	SPR	50 ng/mL	50 ng/mL- 50 μg/mL	60 min	-	39
	SPR	5 ng/mL	-	15 min	-	40
	SPR	0.02 ng/mL	0.03 - 0.5 ng/mL	25 min	drinking water	41
	SPR with MIPS	2 fg/mL	0.2 – 2.0 ng/ml	10 min	-	42
	SPR with MIPS	0.7 ng/mL	0.5- 15 ng/mL	32 min	-	43
	RiFS	0.25 ng/mL	up to 10 ng/mL	30 min	groundwater	44
	MZI	0.1 ng/mL	0.3- 10 ng/mL	10 min	soil	45
	Resonant mirror	1 ng/mL	0.1 ng/mL- 10 μg/mL	5 min	soil	46
	ITO waveguide	0.1 ng/mL	0.1 -100 ng/mL	30 min	-	48
	RAIRS	0.3 ng/mL	up to 10 ng/mL	180 min	-	49
Paraquat	**Proposed sensor**	**0.04 ng/mL**	**0.08-2.5 ng/mL**	**12 min**	**bottled & tap water**	
	Fluoroimmunosensor (RIANA)	0.01 ng/mL 0.06 ng/mL	0.3 - 5.0 ng/mL	15 min	MilliQ water river water	21
	Fluoroimmunosensor	0.06 ng/mL	0.12 - 6.0 ng/mL	30 min	drinking water	22
	SPR	-	51-2829 ng/mL	1 min	buffer	23
	SERS	0.51 ng/mL	up to 257 ng/mL	-	water	24

SERS	0.87 ng/mL	26 ng/mL - 257 μg/mL	-	Pear peel	25
SERS	2.5 ng/mL		-	bottled & tap water, apple & grape juice	26